Heliyon 7 (2021) e06832

Contents lists available at ScienceDirect

Heliyon

journal homepage: www.cell.com/heliyon

Research article

Nonlinear time-history earthquake analysis for steel frames

Phu-Cuong Nguyen [a,*], Thanh-Tuan Tran [a], Trong Nghia-Nguyen [b]

[a] Advanced Structural Engineering Laboratory, Faculty of Civil Engineering, Ho Chi Minh City Open University, Ho Chi Minh City, Viet Nam
[b] Faculty of Civil Engineering, Ho Chi Minh City Open University, Ho Chi Minh City, Viet Nam

ARTICLE INFO

Keywords:
Earthquakes
Fiber plastic hinges
Geometric nonlinearity
Inelasticity
Stability functions
Steel frames

ABSTRACT

This study presents a simple, efficient, accurate method for nonlinear time-history earthquake analysis of spatial steel frames. The proposed new fiber plastic hinge method simulating only one element for each member captures the time-history dynamic behavior of steel frames as accurately as sophisticated plastic zone methods. Stability functions and the geometric stiffness matrix are employed for predicting the second-order effects that aim to minimize computational time and computer resources. Residual stresses are considered through two fiber plastic hinges by assigning initial stress values. A numerical integration procedure using Newmark integration combined with the Newton-Raphson balanced iteration algorithm is developed to find a solution to nonlinear dynamic equilibrium equations of the structural system. Shear deformation effects are also considered in the dynamic analysis. The proposed software, named Direct Advanced Analysis and Design (DAAD), is proved to be accurate and reliable as compared with the analysis results generated by expensive commercial Finite Element Analysis (FEA) software packages. The proposed DAAD program can be improved for performance-based direct design and analysis.

1. Introduction

Over the past thirty years, several researchers have developed advanced methods for analyzing and designing steel frame structures [1, 2, 3, 4, 5, 6, 7, 8, 9, 10, 11, 12, 13, 14, 15, 16, 17, 18, 19, 20, 21]. An advanced analysis method may consider some of the following relevant aspects: geometric nonlinearity, inelasticity of material, nonlinear connections, residual stresses, imperfections, buckling, and others. Researchers have investigated two advanced analysis methods, namely plastic hinge approaches [1, 2, 5, 7, 8, 11, 18, 19, 20, 21] and distributed plasticity approaches [3, 4, 6, 10, 12, 13, 14, 15]. In general, distributed plasticity approaches are more accurate but also more complicated and computationally expensive than plastic hinge approaches [22]. Researchers have mainly focused on developing analysis methods for static problems rather than dynamic problems [9, 12, 14, 18, 23, 24, 25, 26, 27, 28, 29, 30, 31, 32, 33, 34, 35, 36, 37, 38].

Distributed plasticity methods for static problems have been developed by Foley and Vinnakota (1997) [3], Teh and Clarke (1999) [4], Jiang et al. (2002) [6], Nguyen and Kim (2016) [15], and others. By contrast, dynamic problems using distributed plasticity methods are rarely considered; exceptions include recent studies by Nguyen and Kim (2014, 2015) [10,12,14]. In distributed plasticity methods, beam-column members have been meshed into many sub-elements along the member length. Cross-sections of sub-elements have also been meshed into many small fibers. The aim of this work is to monitor the stress-strain relationship of the fibers at each monitoring position of the beam-column members, finally integrating along the member length to obtain the elemental tangent stiffness matrix used for nonlinear analysis. Chiorean (2017) [16], Du et al. (2017) [17], Du et al. (2019) [21], and others have proposed a second-order flexibility-based framed element for direct analysis of steel frames. The work of Du et al. (2019) [21] considers the interaction of initial imperfections, shear deformation, and inelasticity of material simultaneously. They employ Hellinger-Reissner functions for precisely capturing the forces inside the element. The distributed plasticity methods are more accurate, but they are complicated for programming and obtaining convergence in highly nonlinear problems, especially dynamic analysis.

Plastic hinge methods [1, 2, 5, 8, 11, 18, 20] are also called concentrated plasticity approaches. Plastic hinges are often formed at two member ends; the middle segment of the element is always in the elastic regime. Liu et al. (2014) [39,40] proposed a beam-column element with an arbitrarily-located plastic hinge. To reduce

* Corresponding author.
E-mail addresses: cuong.pn@ou.edu.vn, henycuong@gmail.com (P.-C. Nguyen).

https://doi.org/10.1016/j.heliyon.2021.e06832
Received 30 September 2020; Received in revised form 14 November 2020; Accepted 13 April 2021

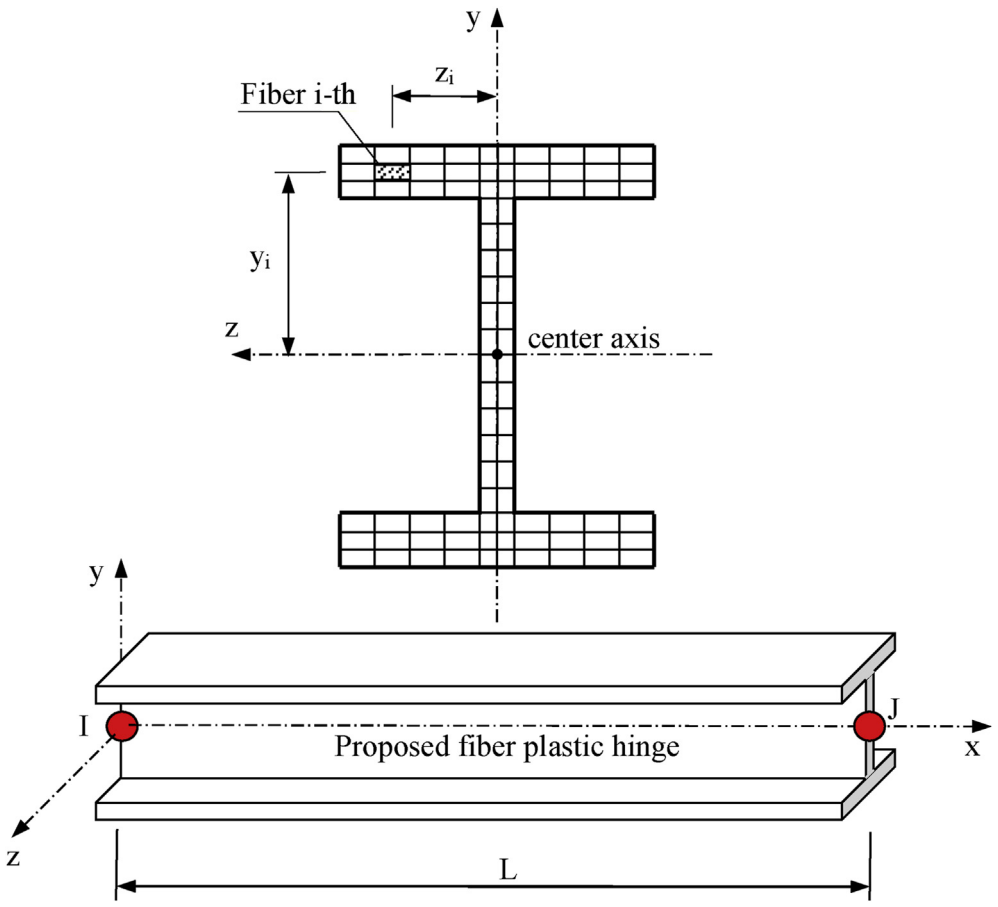

Figure 1. A fiber plastic hinge method.

computational time and resources, stability functions [1, 2, 5, 8, 9, 11, 13, 14, 18, 19, 41, 42] are employed to accurately consider the second-order effects that aim to minimize the analysis modeling. The effects of distributed plasticity, residual stresses, and initial imperfections along the member length are calculated using the tangent modulus concept proposed by King et al. (1992) [1]. Ziemian and McGuire (2002) [43] proposed a novel tangent modulus formulation for capturing the nonlinear static response of steel frames as accurately using the plastic hinge method as the plastic zone method has done. Nguyen and Kim (2012, 2013, 2014, 2015, 2017, 2018) [8,9,11,13,14,18,19] successfully developed software named PAAPS for the advanced analysis of 3D steel frames with semi-rigid connections under static and dynamic loadings. They used stability functions for both the plastic hinge method and the distributed plasticity method; however, in some steel frames under seismic loadings, the results of the analysis cannot converge, and the analysis is interrupted. In this study, a fiber plastic hinge method is improved to overcome existing limitations.

In 1985, Hilmy and Abel [44] presented a graphic program for nonlinear dynamic analysis of 2D steel frames considering second-order effects and material yielding. Nader and Astaneh (1991) [23] carried out

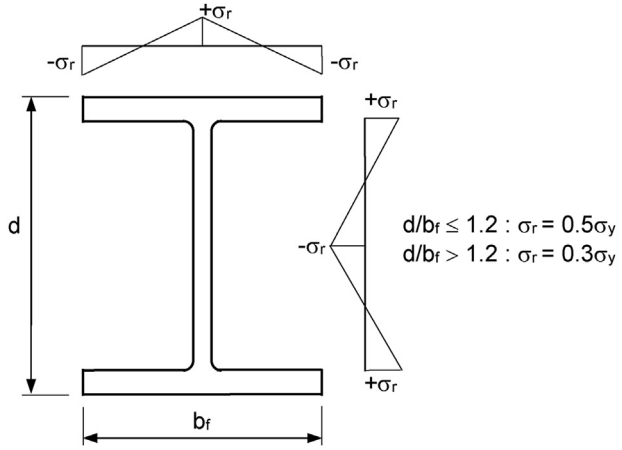

Figure 2. ECCS residual stress pattern.

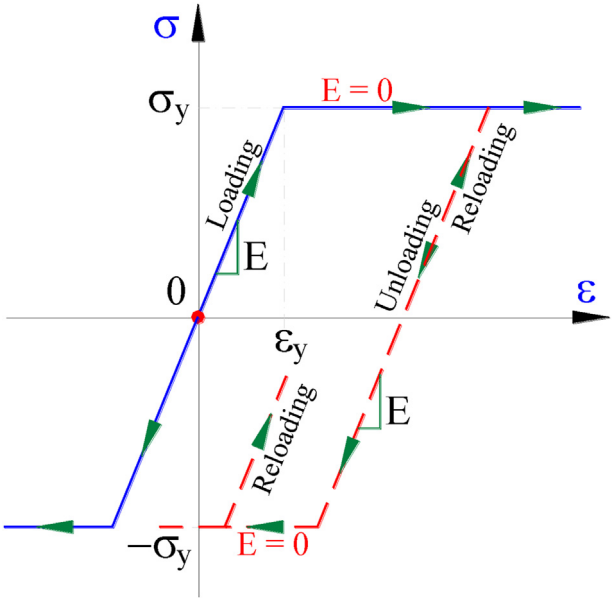

Figure 3. Stress-strain relationship and hysteretic model for steel.

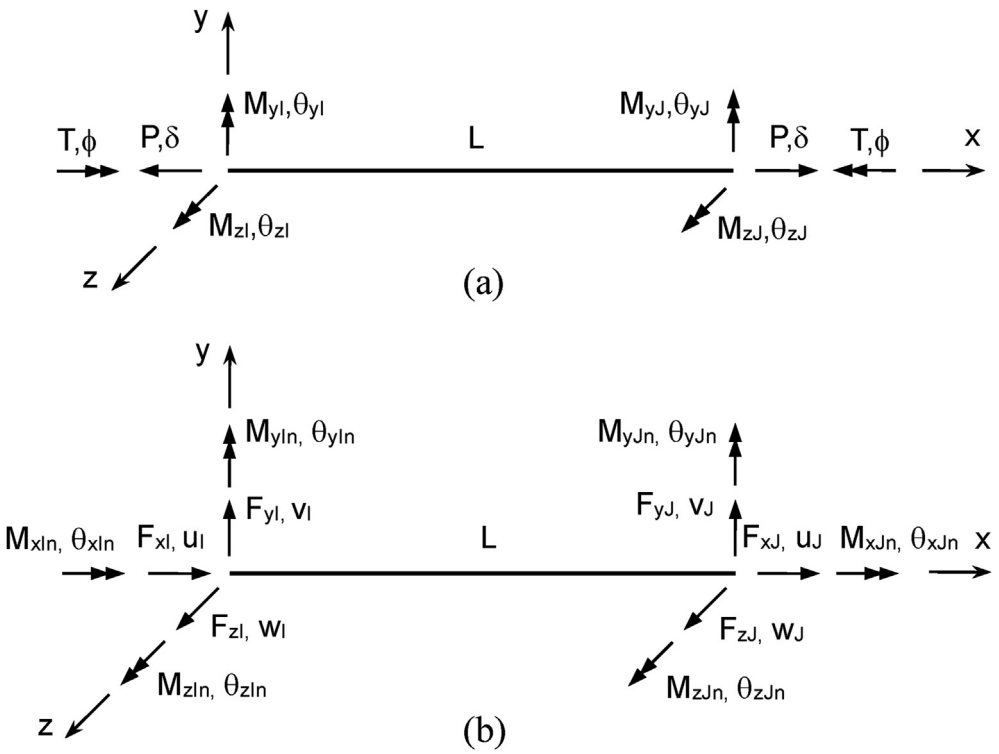

Figure 4. Notations of forces and displacements at two member ends.

44 shaking table tests of past major earthquakes for steel frames with flexible connections. Elnashai and Elghazouli (1994) [24] carried out dynamic tests of two-story steel frames with rigid and semi-rigid connections; they concluded that frames with semi-rigid connections demonstrate ductile and stable hysteretic behavior and can be utilized effectively in earthquake-resistant design. Chen et al. (1997) [25] studied the dynamic behavior of steel frames through shaking table tests. In these tests, beam flanges were shaved around beam-to-column connections. Khudada and Geschwindner (1997) [26] studied the nonlinear dynamic behavior of steel frames using the modal superposition method. In this study, the authors mainly presented the dynamic behavior of the proposed linear and nonlinear panel zone models and linear and nonlinear semi-rigid connections by the spring element. Recently, Sharma et al. (2020) [38] researched dynamic responses of rigid and semi-rigid steel frames under near- and far-field earthquakes.

This study proposes a nonlinear beam-column finite element formulation for predicting the dynamic behavior of spatial steel frames under earthquakes. Stability functions are employed to predict second-order effects, and the geometric stiffness matrix is used to consider the $P-\Delta$ effect. The proposed novel fiber plastic hinge method can accurately and efficiently predict the nonlinear behavior of 3D steel frames utilizing the plastic zone method, but with a simplified formulation. Shear deformation effects and residual stresses are considered simultaneously in the analysis. The Newmark integration method, combined with the Newton-Raphson balanced iteration algorithm, is applied to solve the nonlinear dynamic equations. A proposed program employing the Fortran programming language is developed for predicting the seismic behavior of steel frames. The one element per member modeling approach of the proposed program leads to greater efficiency in computational time and memory use compared with the commercial general finite element software, which uses many small elements per member. The detailed formulations are shown in the next sections.

Table 1. Time steps and peak ground acceleration of earthquakes.

Earthquake	Time step (s)	PGA (g)
El Centro (1940) (Array, #9, USGS Station 117)	0.020	-0.319
Loma Prieta (1989) (Capitola, 000, CDMG Station 47125)	0.005	-0.529
Northridge (1994) (Simi Valley-Katherine, 090, USC Station 90055)	0.010	-0.640
San Fernando (1971) (Pacoima Dam, 254, CDMG Station 279)	0.010	-1.160

2. Nonlinear beam-column element

2.1. $P-\delta$ effects

Chen and Lui [41] and Ekhande et al. [42] proposed stability functions for predicting the $P-\delta$ effects accurately by using one element per beam-column member. The $P-\delta$ effects are the impact of the axial force on bending moments, and moments are increased by axial force. This physical phenomenon is also called a second-order effect. Such an approach minimizes the number of elements (one element per member) and computer resources and saves computational time. The equilibrium equation for a spatial beam-column element is written as follows

$$\begin{Bmatrix} \Delta P \\ \Delta M_{yI} \\ \Delta M_{yJ} \\ \Delta M_{zI} \\ \Delta M_{zJ} \\ \Delta T \end{Bmatrix} = \frac{1}{L} \begin{bmatrix} EA & 0 & 0 & 0 & 0 & 0 \\ 0 & S_{y1}EI_y & S_{y2}EI_y & 0 & 0 & 0 \\ 0 & S_{y2}EI_y & S_{y1}EI_y & 0 & 0 & 0 \\ 0 & 0 & 0 & S_{z1}EI_z & S_{z2}EI_z & 0 \\ 0 & 0 & 0 & S_{z2}EI_z & S_{z1}EI_z & 0 \\ 0 & 0 & 0 & 0 & 0 & GJ \end{bmatrix} \begin{Bmatrix} \Delta\delta \\ \Delta\theta_{yI} \\ \Delta\theta_{yJ} \\ \Delta\theta_{zI} \\ \Delta\theta_{zJ} \\ \Delta\varphi \end{Bmatrix} \quad (1)$$

where S_{y1}, S_{y2}, S_{z1} and S_{z2} are the stability functions proposed by Chen and Lui [41]; E is Young's modulus of steel; G is the shear modulus of steel; A is the area of the cross-section; L is the length of a beam-column element; J is the torsional constant of the cross-section; I_n is the moment of inertia about the n axes $(n = y, z)$; ΔP, ΔM_{yA}, ΔM_{yB}, ΔM_{zA}, ΔM_{zB}, and ΔT are the incremental axial force, the moments at two ends of an element about the y and z axes, and torsion, respectively; and $\Delta\delta$, $\Delta\theta_{yA}$, $\Delta\theta_{yB}$, $\Delta\theta_{zA}$, $\Delta\theta_{zB}$, and $\Delta\varphi$ are the incremental axial displacement, joint rotations, and angle of twist, respectively.

2.2. Proposed fiber plastic hinge

In this section, a novel fiber plastic hinge element is presented. This approach can also be applied to nonlinear analyses of concrete and composite framed structures. In this approach, two fiber plastic hinges are assumed to gradually appear at two member ends, as illustrated in Figure 1, under the impact of external forces. By discretizing cross-sections into many fibers, initial residual stresses are assigned easily. The equilibrium equation for a three-dimensional beam-column element, using stability functions and considering the inelasticity of the material, is written in the incremental form of the force-displacement relationship, as presented below:

$$\begin{Bmatrix} \Delta P \\ \Delta M_{yI} \\ \Delta M_{yJ} \\ \Delta M_{zI} \\ \Delta M_{zJ} \\ \Delta T \end{Bmatrix} = \begin{bmatrix} EA/L & 0 & 0 & 0 & 0 \\ 0 & k_{yii} & k_{yij} & 0 & 0 \\ 0 & k_{yij} & k_{yjj} & 0 & 0 \\ 0 & 0 & 0 & k_{zii} & k_{zij} \\ 0 & 0 & 0 & k_{zij} & k_{zjj} \\ 0 & 0 & 0 & 0 & GJ/L \end{bmatrix} \begin{Bmatrix} \Delta\delta \\ \Delta\theta_{yI} \\ \Delta\theta_{yJ} \\ \Delta\theta_{zI} \\ \Delta\theta_{zJ} \\ \Delta\varphi \end{Bmatrix} \quad (2)$$

where

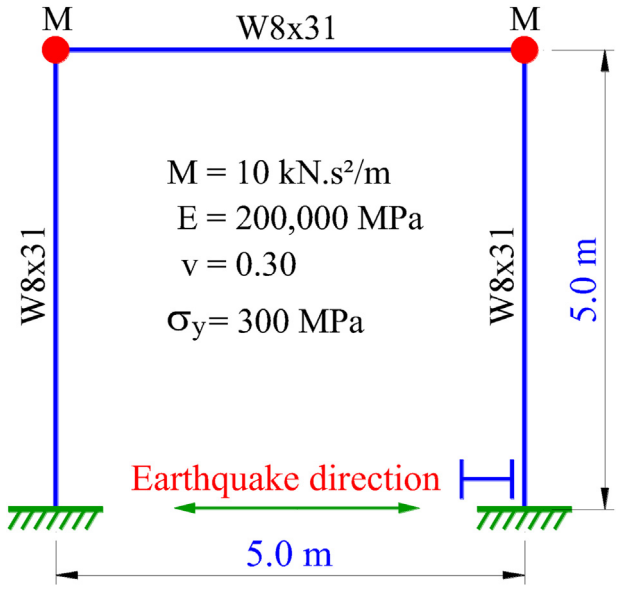

Figure 6. Portal steel frame under earthquakes.

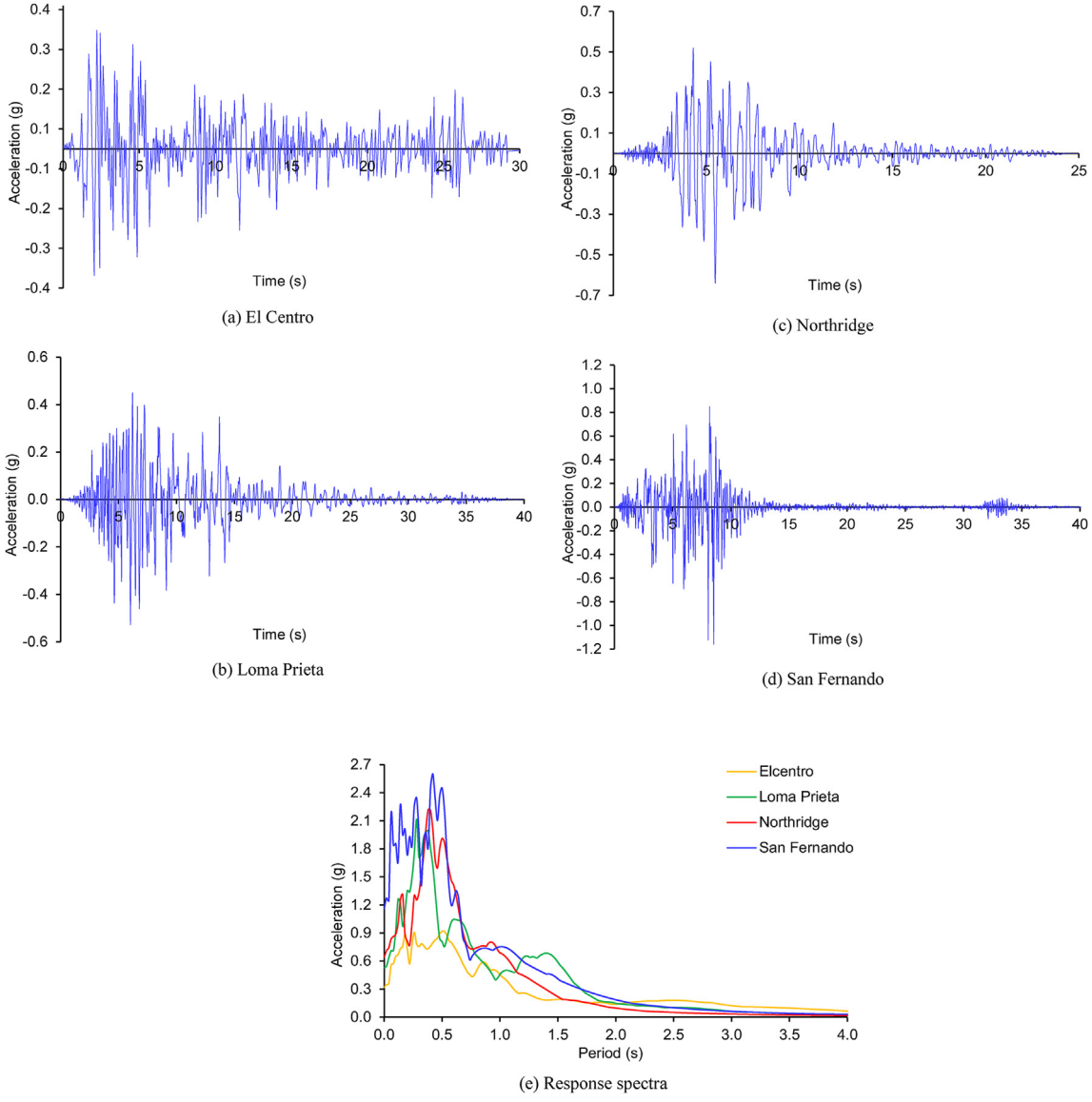

Figure 5. Time-history ground motion and corresponding response spectra of earthquakes (a. El Centro; b. Loma Prieta; c. Northridge; d. San Fernando; e. Response spectra).

Table 2. Modal analysis and Rayleigh damping parameters for the portal frame.

Program	1st period (s)	2nd period (s)	ξ	α_M	β_K
ABAQUS	0.81619	0.029069	0.05	0.74334	$44.67*10^{-5}$
DAAD	0.82145	0.029136	0.05	0.73869	$44.78*10^{-5}$
Diff. (%)	0.64	0.23	0.00	-0.63	0.25

$$k_{yii} = \eta_{yI}\left(S_{y1} - \frac{S_{y2}^2}{S_{y1}}(1-\eta_{yJ})\right)\frac{EI_y}{L} \tag{3}$$

$$k_{yij} = \eta_{yI}\eta_{yJ}S_{y2}\frac{EI_y}{L} \tag{4}$$

$$k_{yjj} = \eta_{yJ}\left(S_{y1} - \frac{S_{y2}^2}{S_{y1}}(1-\eta_{yI})\right)\frac{EI_y}{L} \tag{5}$$

$$k_{zii} = \eta_{zI}\left(S_{z1} - \frac{S_{z2}^2}{S_{z1}}(1-\eta_{zJ})\right)\frac{EI_z}{L} \tag{6}$$

$$k_{zij} = \eta_{zI}\eta_{zJ}S_{z2}\frac{EI_z}{L} \tag{7}$$

$$k_{zjj} = \eta_{zJ}\left(S_{z1} - \frac{S_{z2}^2}{S_{z1}}(1-\eta_{zI})\right)\frac{EI_z}{L} \tag{8}$$

η_{yI}, η_{yJ}, η_{zI}, and η_{zJ} are parameters considering the gradual yielding of hinges. These parameters vary from 1.0 for fully plastic to 0.0 for fully elastic. They are expressed as

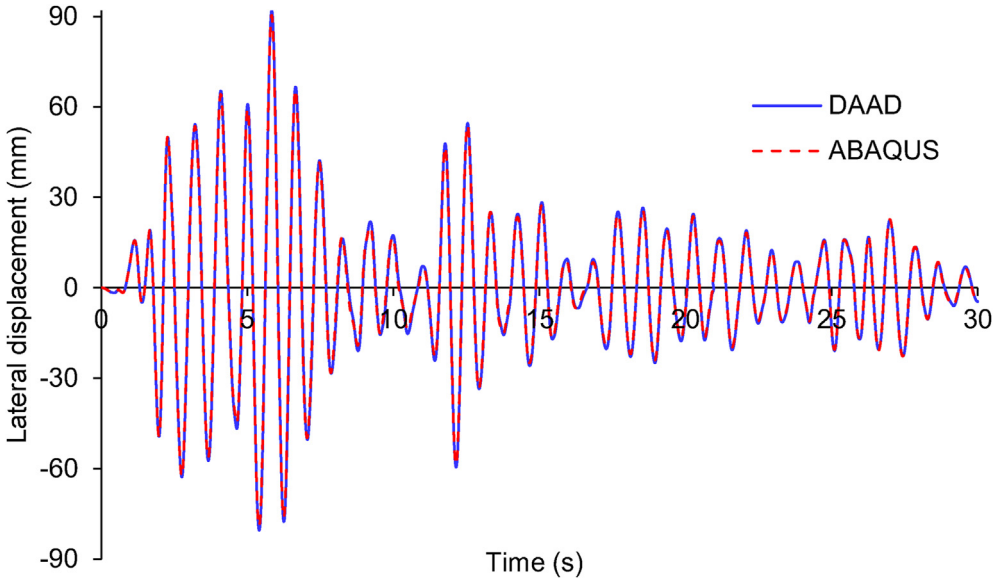

(a) Nonlinear elastic analysis

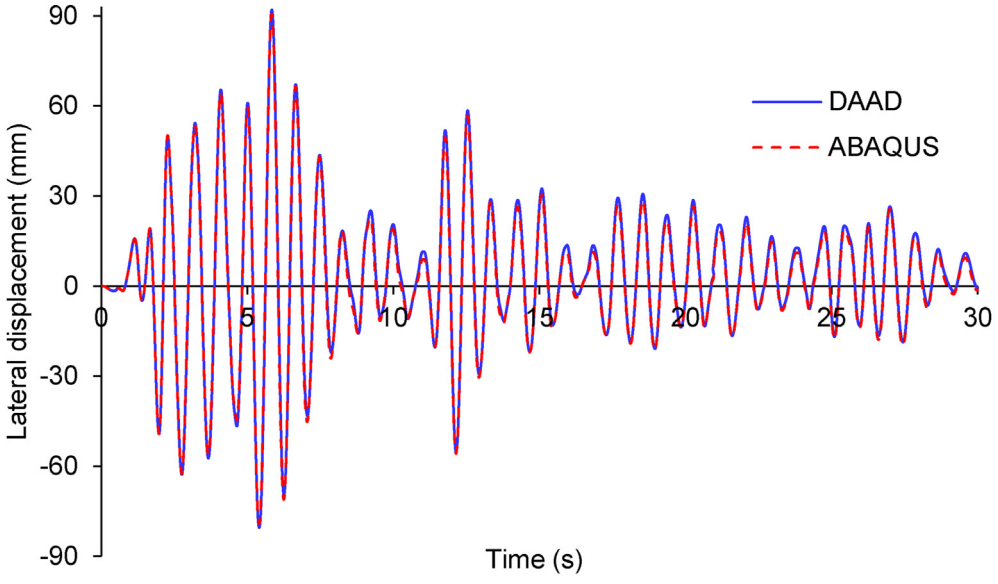

(b) Nonlinear inelastic analysis

Figure 7. Time-history displacement responses of the portal frame under El Centro earthquake (a. Nonlinear elastic analysis; b. Nonlinear inelastic analysis).

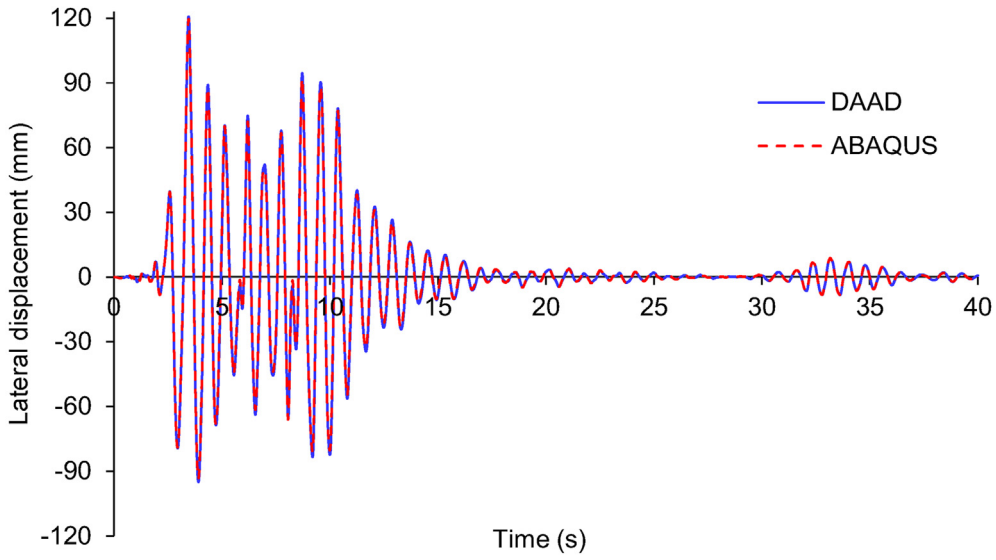

(a) Nonlinear elastic analysis

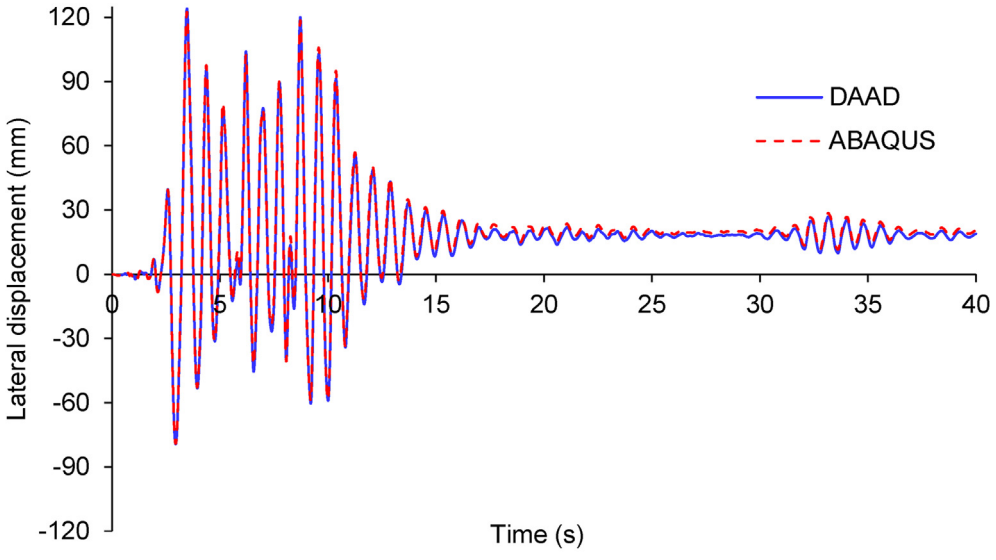

(b) Nonlinear inelastic analysis

Figure 8. Time-history displacement responses of the portal frame under San Fernando earthquake (a. Nonlinear elastic analysis; b. Nonlinear inelastic analysis).

$$\eta_{yI} = \frac{\sum_{i=1}^{m} E_{Ii}\left(A_i z_i^2 + I_{yi}\right)}{EI_y} \tag{9}$$

$$\eta_{yJ} = \frac{\sum_{i=1}^{m} E_{Ji}\left(A_i z_i^2 + I_{yi}\right)}{EI_y} \tag{10}$$

$$\eta_{zI} = \frac{\sum_{i=1}^{m} E_{Ii}\left(A_i y_i^2 + I_{zi}\right)}{EI_z} \tag{11}$$

$$\eta_{zJ} = \frac{\sum_{i=1}^{m} E_{Ji}\left(A_i y_i^2 + I_{zi}\right)}{EI_z} \tag{12}$$

where m is the index considering the cross-section divided into many small fibers; E_{Ii} and E_{Ji} are the tangent Young's moduli of the i^{th} fiber at the two ends I and J, respectively, E_{Ii} and E_{Ji} are equal to zero when the fibers are yielding, and if the fibers are in the elastic behavior regime, E_{Ii} and E_{Ji} are equal to E; A_i is the rectangular area of the i^{th} fiber; I_{yi} and I_{zi} are the y-axis moment of inertia and the z-axis moment of inertia of the i^{th} rectangular fiber around its center axis; and y_i and z_i are the center position of the i^{th} fiber, as presented in Figure 1.

For the I-shape hot-rolled section, the ECCS residual stress pattern [45] shown in Figure 2 is initially inputted to fibers. The elastic-perfectly plastic model and the isotropic hardening rule are assumed for steel materials subjected to cyclic loadings, as shown in Figure 3.

The state of fibers is an essential algorithm for predicting the gradual plasticity of fiber hinges. It is noted that Nguyen and Kim (2014) [11] employed the refined plastic hinge method for predicting the inelastic behavior of steel frames. The gradual plasticity of members is considered

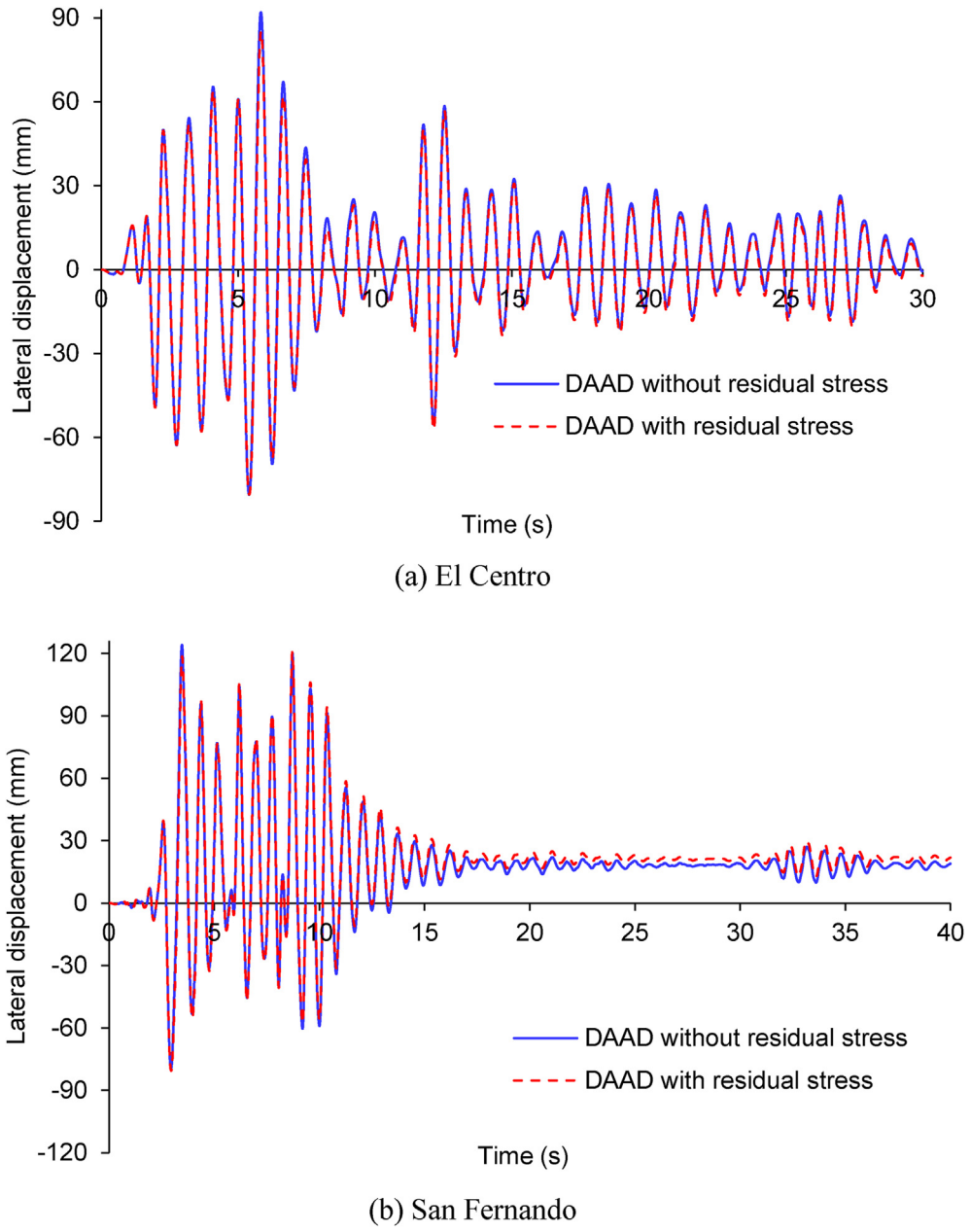

Figure 9. Effects of residual stresses on time-history displacement responses of the portal frame under earthquakes (a. El Centro; b. San Fernando).

by the parabolic function [11] and the yield surface equation proposed by Orbison [46]. In this study, all fibers at the two member ends are monitored (for stress and strain) during the analysis process. Three strain components of deformations are estimated at the fiber hinges: axial strain ε, and curvatures χ_z and χ_y. Section forces and deformations are rewritten in the form of vectors as

$$\text{Section forces } \{S\} = [N \quad M_y \quad M_z]^T \tag{13}$$

$$\text{Section deformations } \{D\} = [\varepsilon \quad \chi_y \quad \chi_z]^T \tag{14}$$

The incremental section forces $\{\Delta S\}$ at the fiber hinges are estimated using the force interpolation matrix $[H(x)]$ as

$$\{\Delta S\} = [H(x)]\{\Delta F\} \tag{15}$$

Table 3. Peak displacements (mm) of the portal frame.

Earthquake	Max/Min	Analysis type	ABAQUS	Present	Error (%)
El Centro	Max	Elastic	90.34	91.84	1.67
		Inelastic	90.42	91.93	1.67
		Inelastic-RS		85.09	-7.44
	Min	Elastic	-79.11	-80.49	1.75
		Inelastic	-79.11	-80.49	1.75
		Inelastic-RS		-80.33	-0.20
San Fernando	Max	Elastic	119.48	120.63	0.97
		Inelastic	122.45	124.03	1.30
		Inelastic-RS		120.76	-2.64
	Min	Elastic	-93.45	-94.93	1.59
		Inelastic	-79.05	-79.35	0.38
		Inelastic-RS		-80.53	1.49

Note: Nonlinear Elastic analysis (Elastic), Nonlinear Inelastic analysis (Inelastic), Nonlinear Inelastic analysis including Residual Stress (Inelastic-RS).

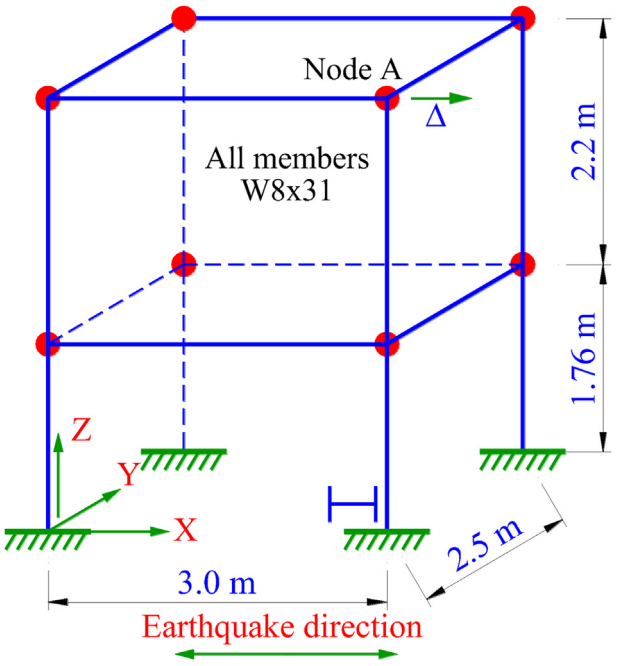

Figure 10. Two-story spatial steel frame under earthquakes.

Table 4. Modal analysis and Rayleigh damping parameters for the two-story spatial frame.

Program	1st period (s)	2nd period (s)	ξ	α_M	β_K
SAP2000 v22	0.98492	0.29493	0.05	0.49093	$36.12*10^{-4}$
DAAD	0.99036	0.29645	0.05	0.48828	$36.31*10^{-4}$
Diff. (%)	0.55	0.52	0.00	-0.54	0.53

$$[H(x)] = \begin{bmatrix} 1 & 0 & 0 & 0 & 0 & 0 \\ 0 & (x/L-1) & x/L & 0 & 0 & 0 \\ 0 & 0 & 0 & (x/L-1) & x/L & 0 \end{bmatrix} \tag{16}$$

where x = L and x = 0 for positions of the fiber hinges at the two ends J and I.

The section deformation is calculated by multiplying the inverse of the sectional stiffness matrix $[k_{sec}]$ by the section forces $\{\Delta S\}$ as

$$\{\Delta D\} = [k_{sec}]^{-1}\{\Delta S\} \tag{17}$$

in which $[k_{sec}]$ is the stiffness matrix of the section at the monitoring end formulated as

$$[k_{sec}] = \begin{bmatrix} \sum_{i=1}^{m} E_i A_i & \sum_{i=1}^{m} E_i A_i z_i & -\sum_{i=1}^{m} E_i A_i y_i \\ \sum_{i=1}^{m} E_i A_i z_i & \sum_{i=1}^{m} E_i (A_i z_i^2 + I_{yi}) & -\sum_{i=1}^{m} E_i A_i y_i z_i \\ -\sum_{i=1}^{m} E_i A_i y_i & -\sum_{i=1}^{m} E_i A_i y_i z_i & \sum_{i=1}^{m} E_i (A_i y_i^2 + I_{zi}) \end{bmatrix} \tag{18}$$

where E_i is the elastic modulus of the i[th] fiber, and the value of E_i is calculated as E_{Ii} or E_{Ji}.

The longitudinal strain of fibers $\{\Delta e\}$ is calculated by the geometric matrix and the incremental section deformation as

$$\{\Delta e\} = \begin{bmatrix} 1 & z_1 & -y_1 \\ 1 & z_2 & -y_2 \\ \dots & \dots & \dots \\ 1 & z_m & -y_m \end{bmatrix} \{\Delta D\} \tag{19}$$

Based on Eq. (19), the total and incremental fiber stresses are estimated by the stress-strain relationship of steel, as shown in Figure 3. Internal forces at fiber hinges are calculated as follows:

$$\{S_R\} = \begin{Bmatrix} N \\ M_y \\ M_z \end{Bmatrix} = \begin{Bmatrix} \sum_{i=1}^{m} \sigma_i A_i \\ \sum_{i=1}^{m} \sigma_i A_i z_i \\ -\sum_{i=1}^{m} \sigma_i A_i y_i \end{Bmatrix} \tag{20}$$

2.3. Shear deformation effects

The coefficients of bending moments in the element stiffness matrix are modified to consider the effects of shear deformation. The equilibrium equation for a three-dimensional beam-column element using stability functions, considering the inelasticity of the material and the effects of shear deformation, is written in the incremental form of the force-displacement relationship as follows:

$$\begin{Bmatrix} \Delta P \\ \Delta M_{yI} \\ \Delta M_{yJ} \\ \Delta M_{zI} \\ \Delta M_{zJ} \\ \Delta T \end{Bmatrix} = \begin{bmatrix} EA/L & 0 & 0 & 0 & 0 & 0 \\ 0 & D_{iiy} & D_{ijy} & 0 & 0 & 0 \\ 0 & D_{ijy} & D_{jjy} & 0 & 0 & 0 \\ 0 & 0 & 0 & D_{iiz} & D_{ijz} & 0 \\ 0 & 0 & 0 & D_{ijz} & D_{jjz} & 0 \\ 0 & 0 & 0 & 0 & 0 & GJ/L \end{bmatrix} \begin{Bmatrix} \Delta\delta \\ \Delta\theta_{yI} \\ \Delta\theta_{yJ} \\ \Delta\theta_{zI} \\ \Delta\theta_{zJ} \\ \Delta\varphi \end{Bmatrix} \tag{21}$$

where

$$D_{iiy} = \frac{k_{iiy}k_{jjy} - k_{ijy}^2 + k_{iiy}A_{sz}GL}{k_{iiy} + k_{jjy} + 2k_{ijy} + A_{sz}GL} \tag{22}$$

$$D_{ijy} = \frac{-k_{iiy}k_{jjy} + k_{ijy}^2 + k_{ijy}A_{sz}GL}{k_{iiy} + k_{jjy} + 2k_{ijy} + A_{sz}GL} \tag{23}$$

$$D_{jjy} = \frac{k_{iiy}k_{jjy} - k_{ijy}^2 + k_{jjy}A_{sz}GL}{k_{iiy} + k_{jjy} + 2k_{ijy} + A_{sz}GL} \tag{24}$$

$$D_{iiz} = \frac{k_{iiz}k_{jjz} - k_{ijz}^2 + k_{iiz}A_{sy}GL}{k_{iiz} + k_{jjz} + 2k_{ijz} + A_{sy}GL} \tag{25}$$

$$D_{ijz} = \frac{-k_{iiz}k_{jjz} + k_{ijz}^2 + k_{ijz}A_{sy}GL}{k_{iiz} + k_{jjz} + 2k_{ijz} + A_{sy}GL} \tag{26}$$

$$D_{jjz} = \frac{k_{iiz}k_{jjz} - k_{ijz}^2 + k_{jjz}A_{sy}GL}{k_{iiz} + k_{jjz} + 2k_{ijz} + A_{sy}GL} \tag{27}$$

in which A_{sy} and A_{sz} are the areas subjected to shear.

2.4. $P-\Delta$ effects

To consider the P-Δ effects, the geometric stiffness matrix is utilized. Figure 4 illustrates a spatial beam-column element with twelve degrees of freedom. The equilibrium and kinematic relationships can be expressed as follows:

$$\{f_n\} = [T]_{6\times12}^{T}\{f_e\} \tag{28}$$

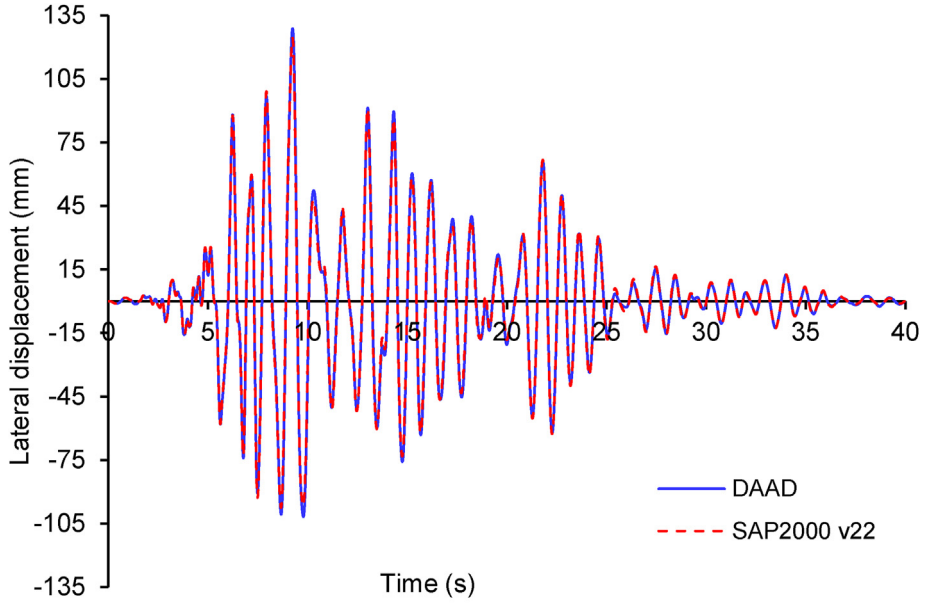

(a) Nonlinear elastic analysis

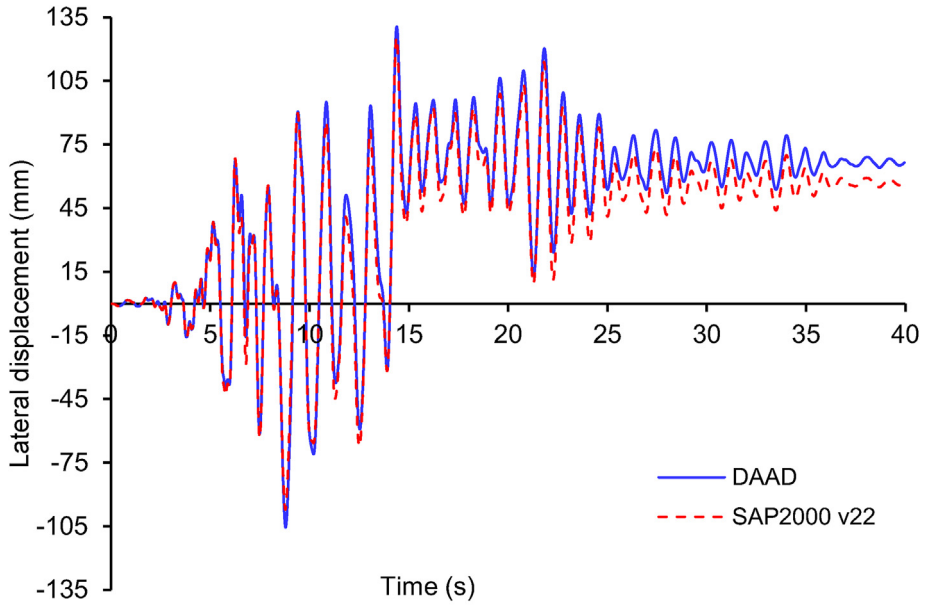

(b) Nonlinear inelastic analysis

Figure 11. Time-history displacement responses of the two-story spatial frame at node A in the X direction under Loma Prieta earthquake (a. Nonlinear elastic analysis; b. Nonlinear inelastic analysis).

$$\{d_e\} = [T]_{6\times12}\{d_L\} \tag{29}$$

where $\{f_n\}$ and $\{d_L\}$ are the incremental end force and displacement vectors of a beam-column element expressed as

$$\{f_n\}^T = \{F_{xI} \;\; F_{yI} \;\; F_{zI} \;\; M_{xIn} \;\; M_{yIn} \;\; M_{zIn} \;\; F_{xJ} \;\; F_{yJ} \;\; F_{zJ} \;\; M_{xJn} \;\; M_{yJn} \;\; M_{zJn}\} \tag{30}$$

$$\{d_L\}^T = \{u_I \;\; v_I \;\; w_I \;\; \theta_{xIn} \;\; \theta_{yIn} \;\; \theta_{zIn} \;\; u_J \;\; v_J \;\; w_J \;\; \theta_{xJn} \;\; \theta_{yJn} \;\; \theta_{zJn}\} \tag{31}$$

and the coordinate transformation matrix $[T]_{6\times12}$ for the framework element is calculated as

$$[T]_{6\times12} = \begin{bmatrix} -1 & 0 & 0 & 0 & 0 & 0 & 1 & 0 & 0 & 0 & 0 & 0 \\ 0 & 0 & -1/L & 0 & 1 & 0 & 0 & 0 & 1/L & 0 & 0 & 0 \\ 0 & 0 & -1/L & 0 & 0 & 0 & 0 & 0 & 1/L & 0 & 1 & 0 \\ 0 & 1/L & 0 & 0 & 0 & 1 & 0 & -1/L & 0 & 0 & 0 & 0 \\ 0 & 1/L & 0 & 0 & 0 & 0 & 0 & -1/L & 0 & 0 & 0 & 1 \\ 0 & 0 & 0 & 1 & 0 & 0 & 0 & 0 & 0 & -1 & 0 & 0 \end{bmatrix} \tag{32}$$

The element force vector is formulated as

$$\{f_n\} = [T]^T_{6\times12}[K_e]_{6\times6}[T]_{6\times12}\{d_L\} \tag{33}$$

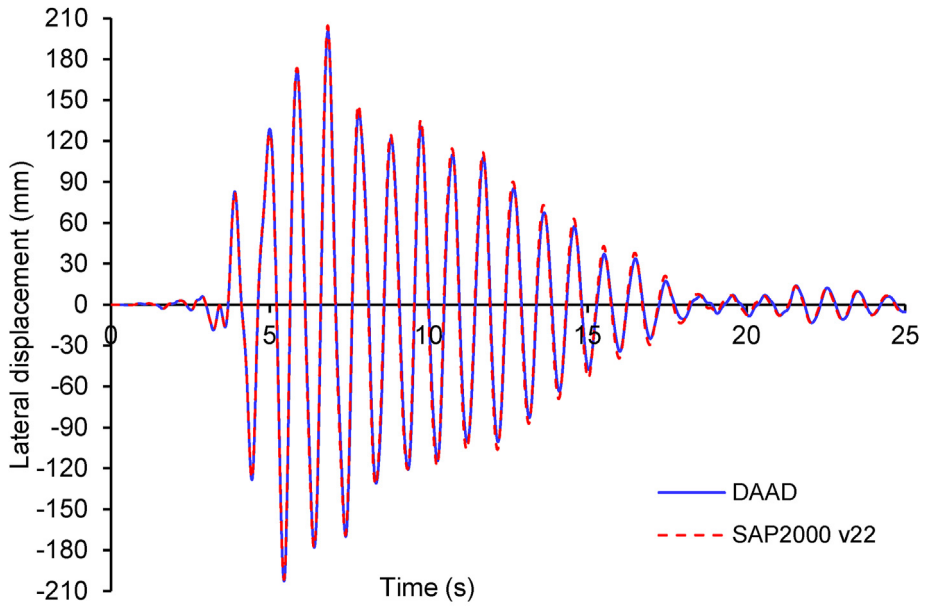

(a) Nonlinear elastic analysis

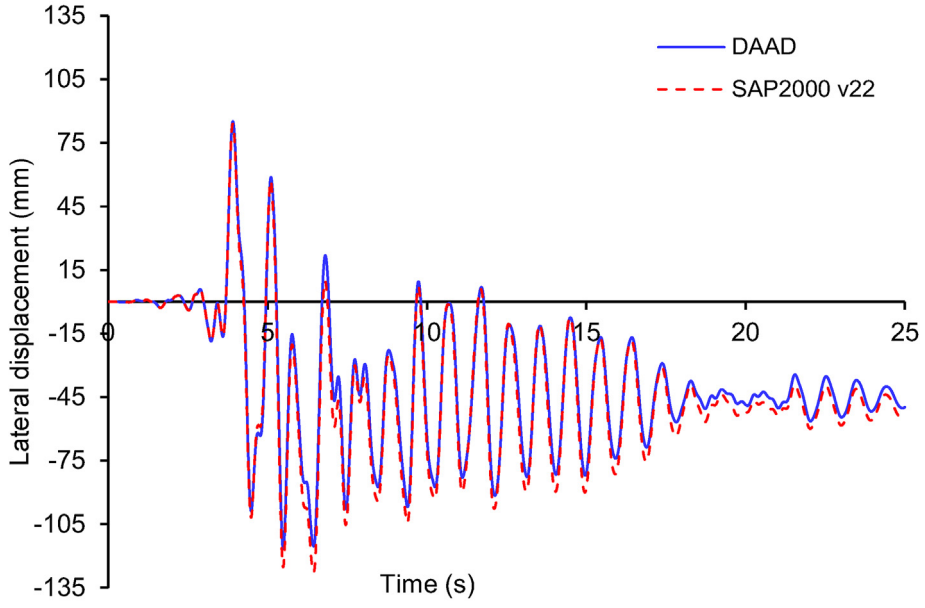

(b) Nonlinear inelastic analysis

Figure 12. Time-history displacement responses of the two-story spatial frame at node A in the X direction under Northridge earthquake (a. Nonlinear elastic analysis; b. Nonlinear inelastic analysis).

The geometric stiffness matrix $[K_g]$ is employed to consider the P-Δ effect. The equilibrium equation is written as follows:

$$\{f_g\} = [K_g]\{d_L\} \tag{34}$$

in which $[K_g]$ is written as

$$[K_g]_{12\times12} = \begin{bmatrix} [K_s] & -[K_s] \\ -[K_s]^T & [K_s] \end{bmatrix} \tag{35}$$

where

$$[K_s] = \begin{bmatrix} 0 & a & -b & 0 & 0 & 0 \\ a & c & 0 & 0 & 0 & 0 \\ -b & 0 & c & 0 & 0 & 0 \\ 0 & 0 & 0 & 0 & 0 & 0 \\ 0 & 0 & 0 & 0 & 0 & 0 \\ 0 & 0 & 0 & 0 & 0 & 0 \end{bmatrix} \tag{36}$$

$$a = \frac{M_{zI} + M_{zJ}}{L^2},\ b = \frac{M_{yI} + M_{yJ}}{L^2},\ c = \frac{P}{L} \tag{37}$$

The tangent stiffness matrix of the element is calculated from the combination of Eqs. (33) and (34) as

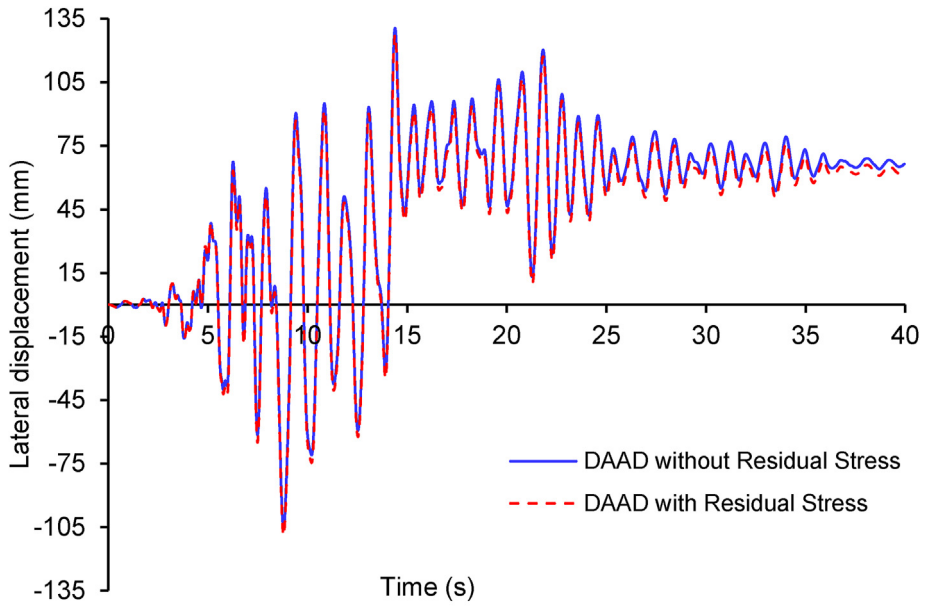

(a) Loma Prieta

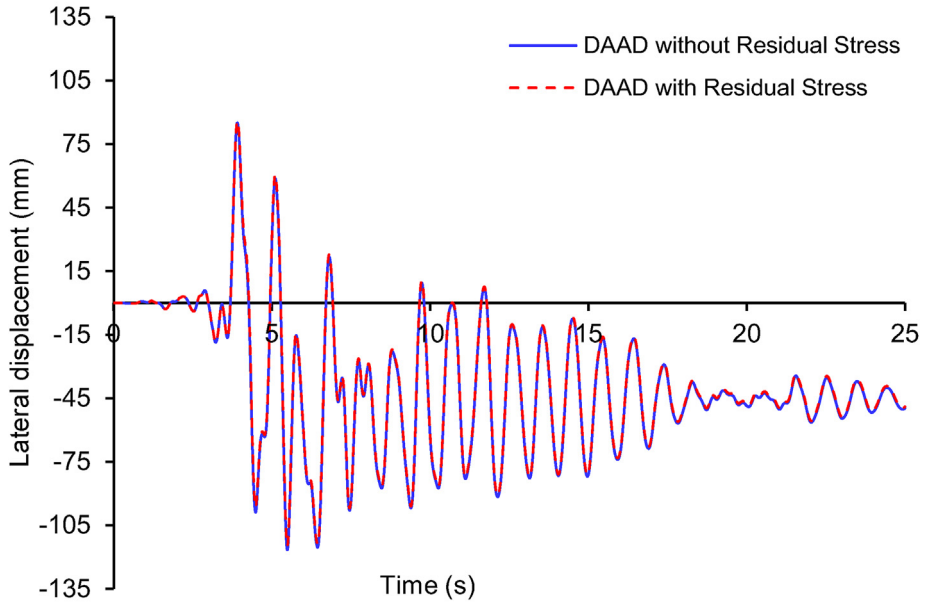

(b) Northridge

Figure 13. Effects of residual stresses on time-history displacement responses of the two-story spatial frame at node A in the X direction under earthquakes (a. Loma Prieta; b. Northridge).

$$[K]_T = [T]^T_{6\times12}[K_e]_{6\times6}[T]_{6\times12} + [K_g]_{12\times12} \quad (38)$$

3. Developed software: DAAD

A software program named Direct Advanced Analysis and Design (DAAD) was developed for the nonlinear time-history earthquake analysis of steel frames. The program solves dynamic problems using Newmark's [47] direct integration method combined with the Newton-Raphson balanced iteration algorithm. It has been verified by commercial Finite Element Analysis (FEA) software such as ABAQUS [48] and SAP2000 [49] version 22. Beam and column members are simulated using one element for both beams and columns using the proposed DAAD program. For a more accurate investigation, all W-sections were divided into 6 × 30 = 180 fibers on each flange and 30 × 2 = 60 fibers for the web; a total of 420 fibers were used for the calculation. All steel materials were assumed to be elastic-perfectly plastic. Time-history acceleration ground motions and corresponding response spectra were collected from the PEER Ground Motion Database [50], as illustrated in Table 1 and Figure 5. The self-weight of structures was neglected in

Table 5. Peak displacements (mm) of the two-story spatial frame.

Earthquake	Max/Min	Analysis type	SAP2000	Present	Error (%)
Loma Prieta	Max	Elastic	124.42	128.79	3.52
		Inelastic	125.41	130.56	4.11
		Inelastic-RS		127.42	-2.41
	Min	Elastic	-97.41	-101.73	4.44
		Inelastic	-97.14	-105.51	8.62
		Inelastic-RS		-108.98	3.29
Northridge	Max	Elastic	204.62	200.65	-1.95
		Inelastic	83.91	85.09	1.41
		Inelastic-RS		85.85	0.89
	Min	Elastic	-201.48	-202.72	0.62
		Inelastic	-127.77	-116.58	-8.76
		Inelastic-RS		-114.72	-1.60

Note: Nonlinear Elastic analysis (Elastic), Nonlinear Inelastic analysis (Inelastic), Nonlinear Inelastic analysis including Residual Stress (Inelastic-RS).

all the analyses. Rayleigh damping [51] was used as the structural viscous damping in the analyses.

4. Verification and discussion

4.1. Portal steel frame under El Centro and San Fernando earthquakes

A portal frame was fabricated using W8x31 sections; its geometric characteristics and material properties are shown in Figure 6. The frame included lumped masses of 10 kNs^2/m at the column tops; the frame was subjected to the El Centro and San Fernando earthquakes, as shown in Figure 5 and Table 1. In this study using the DAAD program, the beam-column member was simulated using only one element per member and was monitored at two ends for plastic hinges. To predict the nonlinear inelastic behavior of the frame accurately, the ABAQUS program [48] must divide the beam-column member into many sub-elements; thus 40 elements per member were used in the time-history analysis. W-sections were meshed into $6 \times 30 = 180$ fibers on each flange and $30 \times 2 = 60$ fibers for the web; a total of 420 fibers were used for calculation in the proposed DAAD program. Rayleigh damping coefficients were estimated using the first two natural vibration modes of the structure and a damping ratio of 0.05, as calculated in Table 2. The results of the vibration periods predicted by ABAQUS and the proposed DAAD program were almost identical, with errors less than 0.65%. The participating mass ratios of the two main vibration modes generated by the proposed program were 0.9999954 and 0.0000046, respectively. Thus, the proposed DAAD program predicted the modal analysis accurately for the portal frame.

By considering Rayleigh damping and ignoring residual stresses in all of the below nonlinear analyses, the time-displacement responses of the frame generated by nonlinear elastic and inelastic analysis by the proposed DAAD program were identical to the results generated by the ABAQUS program, as shown in Figure 7 for the El Centro earthquake and Figure 8 for the San Fernando earthquake. The results matched well with the expensive commercial FEA software ABAQUS.

Analyzing the nonlinear inelastic responses of the frame under the San Fernando earthquake using the same computer configuration (Intel® Core™ i7-7500U CPU @ 2.70GHz; 16.00 GB RAM; 1000.0 GB HDD; Windows 10), the computational times of the proposed DAAD program and ABAQUS were 1 min 55 s and 9 min 48 s, respectively. The computational time of ABAQUS was 5.1 times longer than the proposed program. This result proves the computational efficiency of the proposed DAAD program. However, the computational time obtained by the proposed program depends on the number of divided fibers on the fiber plastic hinges. In this study, a total of 420 fibers were used for each fiber plastic hinge in the analysis. In the ABAQUS modeling, each frame member was divided into forty small elements using the B22 Timoshenko beam element, since ABAQUS cannot accurately predict the nonlinear inelastic responses of the frame if only a few elements per member are used in the modeling.

Figure 9 was drawn by the proposed DAAD program. It shows the effects of residual stresses on the frame's nonlinear inelastic time-displacement responses. Residual stresses do not significantly affect the earthquake behavior of the portal frame. Table 3 shows peak displacements of the portal frame under the conditions of various earthquakes.

4.2. Two-story spatial steel frame under Loma Prieta and Northridge earthquakes

A two-story spatial steel frame was fabricated using all W8x31 sections; its dimensions are shown in Figure 10. Elastic modulus, Poisson's ratio, and the yield stress of steel were 200,000 MPa, 0.30, and 350 MPa, respectively. Lumped masses of 50 kNs^2/m were placed at the column tops. The frame was subjected to the Loma Prieta and Northridge earthquakes in the X-direction. Time-history ground motion records are shown in Figure 5 and Table 1. Using the proposed DAAD program, each beam-column member was simulated using one element per member, while SAP2000 software [49] also used modeling with one element per member for the analysis. All W-sections were divided into $6 \times 30 = 180$ fibers on each flange and $30 \times 2 = 60$ fibers for the web; a total of 420 fibers were used for calculation in the proposed DAAD program. Rayleigh damping coefficients were estimated using the first two natural vibration modes of the structure and a damping ratio of 0.05, as shown in Table 4. The vibration periods and Rayleigh damping parameters generated by the proposed program were similar to those of the SAP2000 program, and the difference was not larger than 0.55%. The participating mass ratios of the two main vibration modes were 0.82135 and 0.17864, generated by SAP2000 v22. Those ratios estimated by the proposed program were 0.82126 and 0.17873. Therefore, the proposed DAAD program predicted the modal analysis accurately for the two-story spatial frame.

By considering Rayleigh damping and ignoring residual stresses in all of the below nonlinear analyses, the time-displacement responses of the frame at node A in the X direction generated by the nonlinear elastic and inelastic analysis of the proposed DAAD program were identical with those of SAP2000, as shown in Figure 11 for the Loma Prieta earthquake and Figure 12 for the Northridge earthquake. The results almost agreed with the expensive commercial software SAP2000. The differences between the results of DAAD and SAP2000 in the nonlinear inelastic

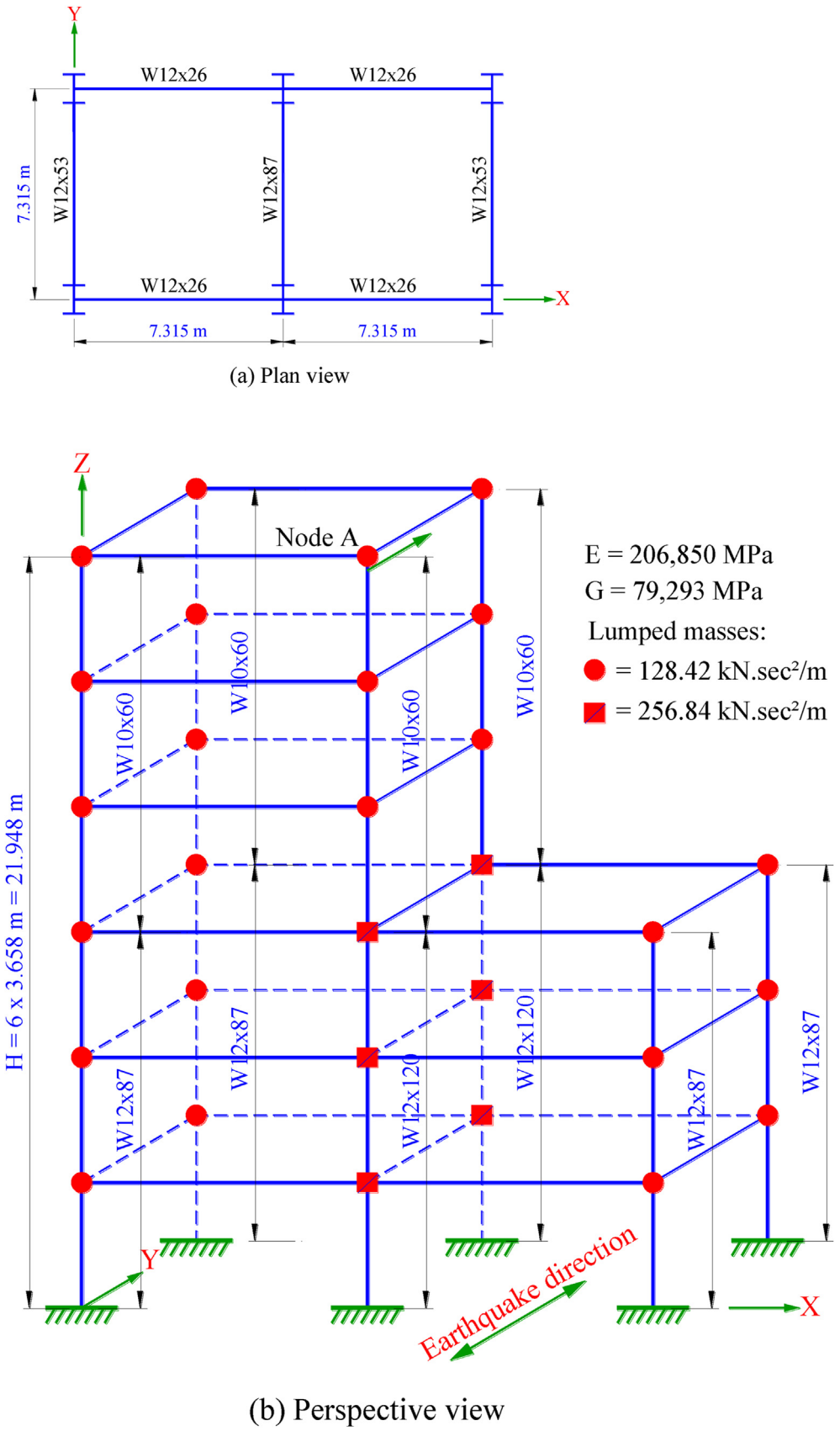

Figure 14. Six-story spatial steel frame under earthquakes (a. Plan view; b. Perspective view).

Table 6. Modal analysis and Rayleigh damping parameters for the six-story spatial frame.

Program	1st period (s)	2nd period (s)	ξ	α_M	β_K
SAP2000 v22	5.53854	1.99584	0.05	0.08339	$23.35*10^{-3}$
DAAD	5.55470	2.00200	0.05	0.08315	$23.42*10^{-3}$
Diff. (%)	0.29	0.31	0.00	-0.29	0.30

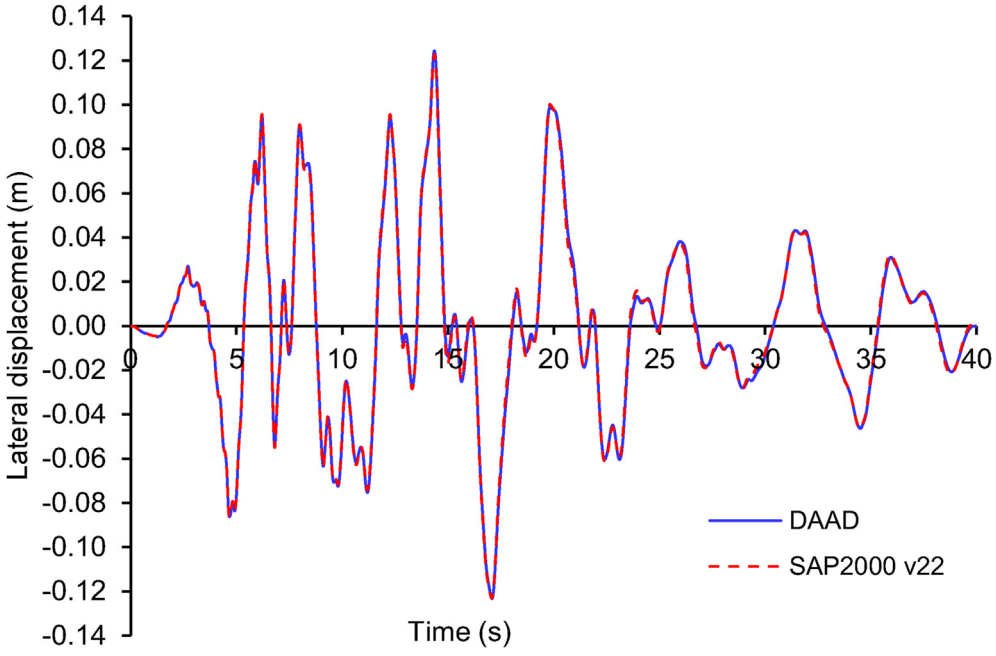

(a) Nonlinear elastic analysis

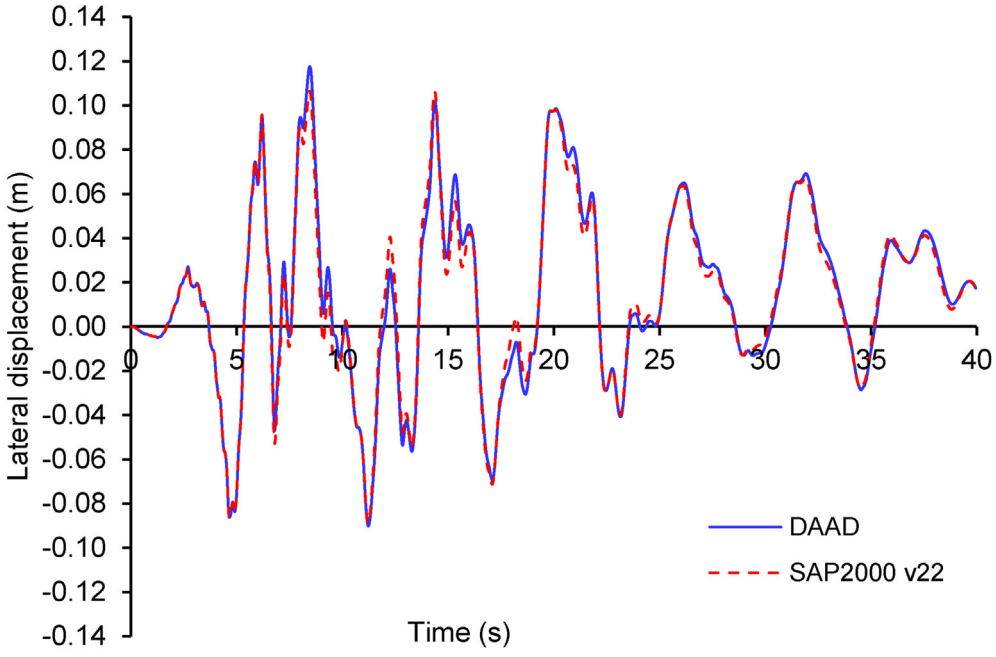

(b) Nonlinear inelastic analysis

Figure 15. Time-history displacement responses of the six-story spatial frame at node A in the Y direction under Loma Prieta earthquake (a. Nonlinear elastic analysis; b. Nonlinear inelastic analysis).

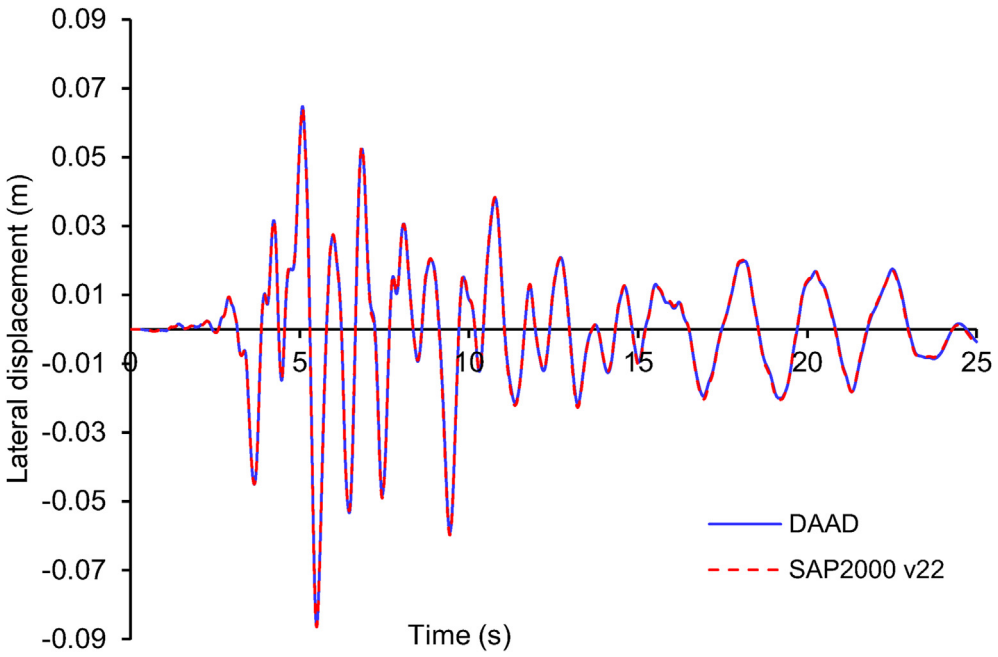

(a) Nonlinear elastic analysis

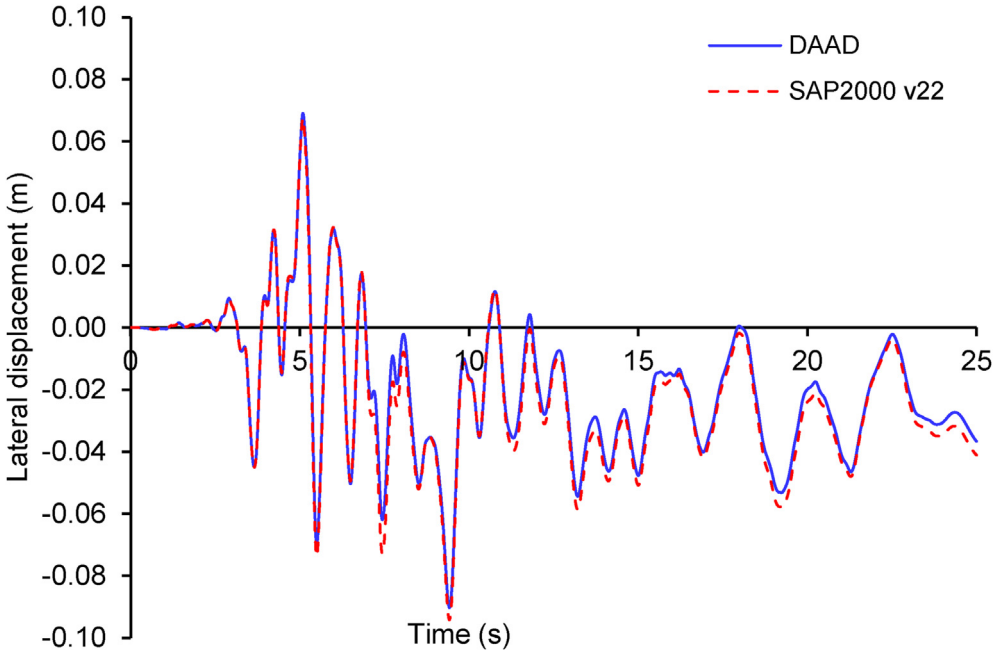

(b) Nonlinear inelastic analysis

Figure 16. Time-history displacement responses of the six-story spatial frame at node A in the Y direction under Northridge earthquake (a. Nonlinear elastic analysis; b. Nonlinear inelastic analysis).

analysis, as shown in Figure 11b and Figure 12b, can be explained by the differences between SAP2000 and DAAD in terms of their plasticity approaches and finite element formulations. SAP2000 uses the hinge interaction surface (P-M2-M3) to consider plastic hinges, while the proposed DAAD program uses the proposed fiber plastic hinge method.

Figure 13 shows the effects of residual stresses on the nonlinear inelastic time-displacement responses of the frame at node A in the X direction generated by the proposed DAAD program. Residual stresses did not significantly affect the earthquake behavior of the two-story spatial frame. Table 5 shows the peak displacements of the two-story spatial frame under various earthquakes.

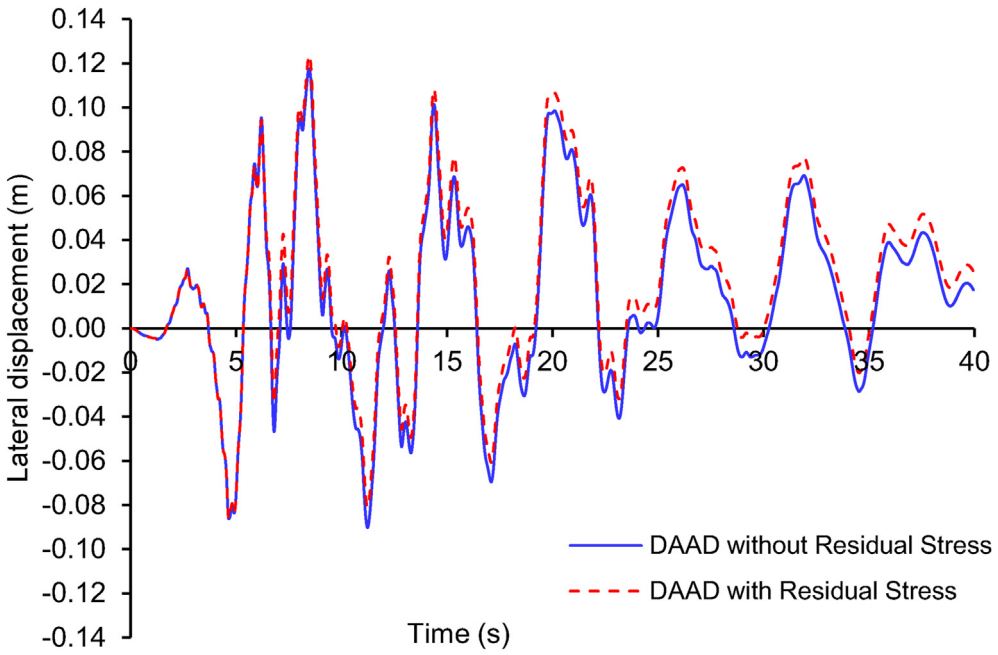

(a) Loma Prieta

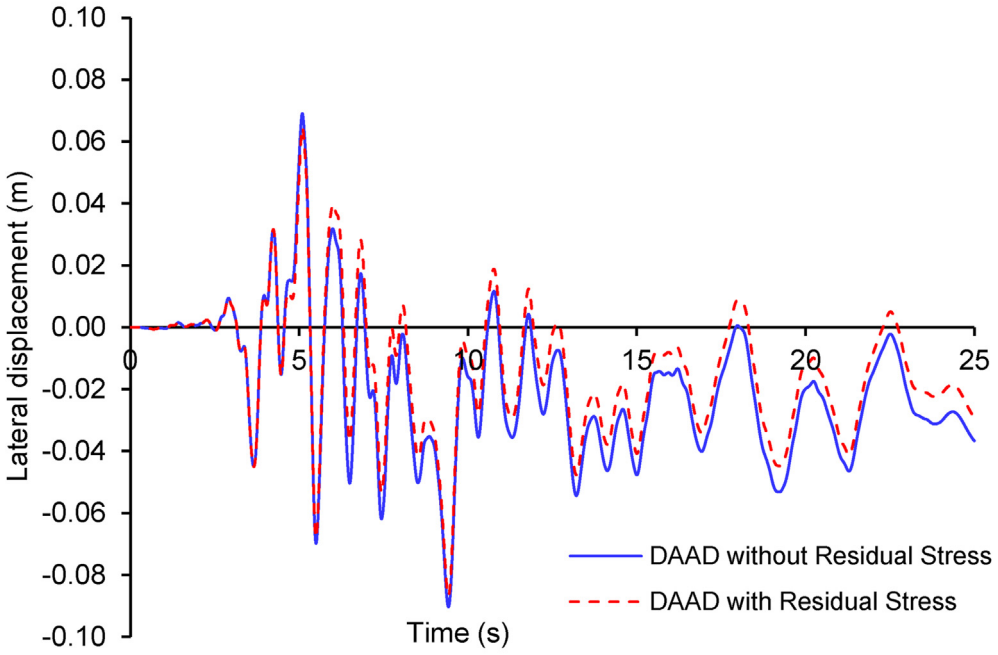

(b) Northridge

Figure 17. Effects of residual stresses on time-history displacement responses of the six-story spatial frame at node A in the Y direction under earthquakes (a. Loma Prieta; b. Northridge).

4.3. Orbison six-story spatial steel frame under Loma Prieta and Northridge earthquakes

An Orbison six-story spatial steel frame was fabricated using all W-sections; its dimensions, material properties, and lumped masses are shown in Figure 14. The yield stress of the steel was 250 MPa. The frame was subjected to the Loma Prieta and Northridge earthquakes in the Y-direction; the loading data are shown in Figure 5 and Table 1. Using the proposed DAAD program, the beam-column member was simulated using one element per member, while SAP2000 also used modeling with one element per member for its analysis. All W-sections were divided into $6 \times 30 = 180$ fibers on each flange and $30 \times 2 = 60$ fibers for the web; a total of 420 fibers were used for calculation in the proposed DAAD program. Rayleigh damping coefficients were estimated using the

Table 7. Peak displacements (mm) of the six-story spatial frame.

Earthquake	Max/Min	Analysis type	SAP2000	Present	Error (%)
Loma Prieta	Max	Elastic	122.71	124.30	1.30
		Inelastic	106.38	117.52	10.48
		Inelastic-RS		123.62	5.19
	Min	Elastic	-86.38	-86.30	-0.10
		Inelastic	-88.99	-90.18	1.34
		Inelastic-RS		-86.30	-4.30
Northridge	Max	Elastic	64.30	64.72	0.66
		Inelastic	67.42	69.03	2.39
		Inelastic-RS		64.48	-6.59
	Min	Elastic	-86.44	-86.12	-0.38
		-*Inelastic	-94.17	-90.30	-4.11
		Inelastic-RS		-86.74	-3.94

Note: Nonlinear Elastic analysis (Elastic), Nonlinear Inelastic analysis (Inelastic), Nonlinear Inelastic analysis including Residual Stress (Inelastic-RS).

first two natural vibration modes of the structure and a damping ratio of 0.05, as shown in Table 6. The proposed DAAD program predicted vibration periods and Rayleigh damping coefficients similar to those of SAP2000; the difference was not larger than 0.31%. The participating mass ratios of the two main vibration modes were 0.54705 and 0.09412, generated by SAP2000 v22. Those ratios estimated by the proposed program were 0.54604 and 0.09454. Thus, the proposed DAAD program predicted the modal analysis accurately for planar and spatial steel frames.

By considering Rayleigh damping and ignoring residual stresses in all of the below nonlinear analyses, the time-displacement responses of the frame at node A in the earthquake Y-direction generated by nonlinear elastic and inelastic analysis of the proposed DAAD program were almost identical with the results generated by the SAP2000 program, as shown in Figure 15 for the Loma Prieta earthquake and Figure 16 for the Northridge earthquake. The results almost agreed with the expensive commercial software SAP2000.

Using the same computer configuration (Intel® Core™ i7-7500U CPU @ 2.70GHz; 16.00 GB RAM; 1000.0 GB HDD; Windows 10), the computational times of the proposed DAAD program and SAP2000 were 15 min 25 s and 25 s, respectively. The computational time of DAAD was longer than SAP2000 version 22 (the newest version). In version 22 of SAP2000, solution algorithms and formulations have improved significantly. SAP2000 uses the hinge interaction surface (P-M2-M3) to consider plastic hinges, while the proposed DAAD program uses the proposed fiber plastic hinge method. The proposed DAAD program's solution algorithm and programming techniques need to be improved in the future.

Figure 17 shows the effects of residual stresses on the nonlinear inelastic time-displacement responses of the frame at node A in the Y direction using the proposed DAAD program. Residual stresses result in a clear tolerance on the six-story spatial frame's earthquake behavior. Table 7 shows the peak displacements of the six-story spatial frame under various earthquakes.

5. Conclusion

A novel fiber plastic hinge method has been presented in detail and has been proved reliable by several quantitative examples using planar and spatial steel frames. The novel fiber plastic hinge method was used to develop the DAAD program (Direct Advanced Analysis and Design). The proposed DAAD program can reliably, efficiently, and accurately simulate the nonlinear inelastic behavior of steel frames subjected to earthquakes using one element each for both beams and columns. Several response modes were taken into account, such as residual stresses, geometric nonlinearity, and the plasticity of steel. The nonlinear solution procedure was developed and coded into the nonlinear inelastic analysis program for steel frames. Initial residual stresses did not significantly affect the time-history displacement behavior of the investigated steel frames. The proposed DAAD program can be utilized for daily practical engineering design. In our next project, we will develop the DAAD program for considering the effects of the panel zone and the flexibility of beam-to-column connections.

Declarations

Author contribution statement

Phu-Cuong Nguyen: Conceived and designed the experiments; Performed the experiments; Analyzed and interpreted the data; Contributed reagents, materials, analysis tools or data; Wrote the paper.

Thanh-Tuan Tran: Performed the experiments; Analyzed and interpreted the data; Contributed reagents, materials, analysis tools or data; Wrote the paper.

Trong Nghia-Nguyen: Conceived and designed the experiments; Performed the experiments; Analyzed and interpreted the data; Wrote the paper.

Funding statement

This work was supported by the Ministry of Education and Training (MOET), VIETNAM (Grant No. B2019–MBS–01).

Data availability statement

Data will be made available on request.

Declaration of interests statement

The authors declare no conflict of interest.

Additional information

No additional information is available for this paper.

Acknowledgements

The authors gratefully acknowledge the financial support granted by the Scientific Research Fund of the Ministry of Education and Training (MOET), Vietnam, under the grant No. B2019–MBS–01. The authors would also like to thank colleagues at Ho Chi Minh City Open University for supporting this project.

References

[1] W.S. King, D.W. White, W.F. Chen, Second-order inelastic analysis methods for steel-frame design, J. Struct. Eng. 118 (1992) 408–428.
[2] S.-E. Kim, W.-F. Chen, Practical advanced analysis for unbraced steel frame design, J. Struct. Eng. 122 (1996) 1259–1265.
[3] C.M. Foley, S. Vinnakota, Inelastic analysis of partially restrained unbraced steel frames, Eng. Struct. 19 (1997) 891–902.
[4] L.H. Teh, M.J. Clarke, Plastic-zone analysis of 3D steel frames using beam elements, J. Struct. Eng. 125 (1999) 1328–1337.
[5] S.-E. Kim, Y. Kim, S.-H. Choi, Nonlinear analysis of 3-D steel frames, Thin-Walled Struct. 39 (2001) 445–461.
[6] X.-M. Jiang, H. Chen, J.Y.R. Liew, Spread-of-plasticity analysis of three-dimensional steel frames, J. Constr. Steel Res. 58 (2002) 193–212.
[7] C.G. Chiorean, A computer method for nonlinear inelastic analysis of 3D semi-rigid steel frameworks, Eng. Struct. 31 (2009) 3016–3033.
[8] C. Ngo-Huu, P.-C. Nguyen, S.-E. Kim, Second-order plastic-hinge analysis of space semi-rigid steel frames, Thin-Walled Struct. 60 (2012) 98–104.
[9] P.-C. Nguyen, S.-E. Kim, Nonlinear elastic dynamic analysis of space steel frames with semi-rigid connections, J. Constr. Steel Res. 84 (2013) 72–81.
[10] P.-C. Nguyen, N.T.N. Doan, C. Ngo-Huu, S.-E. Kim, Nonlinear inelastic response history analysis of steel frame structures using plastic-zone method, Thin-Walled Struct. 85 (2014) 220–233.
[11] P.-C. Nguyen, S.-E. Kim, Nonlinear inelastic time-history analysis of three-dimensional semi-rigid steel frames, J. Constr. Steel Res. 101 (2014) 192–206.
[12] P.-C. Nguyen, S.-E. Kim, Distributed plasticity approach for time-history analysis of steel frames including nonlinear connections, J. Constr. Steel Res. 100 (2014) 36–49.
[13] P.-C. Nguyen, S.-E. Kim, An advanced analysis method for three-dimensional steel frames with semi-rigid connections, Finite Elem. Anal. Des. 80 (2014) 23–32.
[14] P.-C. Nguyen, S.-E. Kim, Second-order spread-of-plasticity approach for nonlinear time-history analysis of space semi-rigid steel frames, Finite Elem. Anal. Des. 105 (2015) 1–15.
[15] P.-C. Nguyen, S.-E. Kim, Advanced analysis for planar steel frames with semi-rigid connections using plastic-zone method, Steel Compos. Struct. 21 (2016) 1121–1144.
[16] C.G. Chiorean, Second-order flexibility-based model for nonlinear inelastic analysis of 3D semi-rigid steel frameworks, Eng. Struct. 136 (2017) 547–579.
[17] Z.-L. Du, Y.-P. Liu, S.-L. Chan, A second-order flexibility-based beam-column element with member imperfection, Eng. Struct. 143 (2017) 410–426.
[18] P.-C. Nguyen, S.-E. Kim, Investigating effects of various base restraints on the nonlinear inelastic static and seismic responses of steel frames, Int. J. Non Lin. Mech. 89 (2017) 151–167.
[19] P.-C. Nguyen, S.-E. Kim, A new improved fiber plastic hinge method accounting for lateral-torsional buckling of 3D steel frames, Thin-Walled Struct. 127 (2018) 666–675.
[20] A.H. Zubydan, A.I. ElSabbagh, T. Sharaf, A.-E. Farag, Inelastic large deflection analysis of space steel frames using an equivalent accumulated element, Eng. Struct. 162 (2018) 121–134.
[21] Z.-L. Du, Z.-X. Ding, Y.-P. Liu, S.-L. Chan, Advanced flexibility-based beam-column element allowing for shear deformation and initial imperfection for direct analysis, Eng. Struct. (2019) 199.
[22] A.S. Elnashai, L. Di Sarno, Fundamentals of Earthquake Engineering, Wiley Online Library, 2008.
[23] M. Nader, A. Astaneh, Dynamic behavior of flexible, semirigid and rigid steel frames, J. Constr. Steel Res. 18 (1991) 179–192.
[24] A. Elnashai, A. Elghazouli, Seismic behaviour of semi-rigid steel frames, J. Constr. Steel Res. 29 (1994) 149–174.
[25] S.-J. Chen, J. Chu, Z. Chou, Dynamic behavior of steel frames with beam flanges shaved around connection, J. Constr. Steel Res. 42 (1997) 49–70.
[26] A. Khudada, L. Geschwindner, Nonlinear dynamic analysis of steel frames by modal superposition, J. Struct. Eng. 123 (1997) 1519–1527.
[27] A. Reyes-Salazar, A. Haldar, Seismic response and energy dissipation in partially restrained and fully restrained steel frames: an analytical study, Steel Compos. Struct. 1 (2001) 459–480.
[28] M. Sekulovic, R. Salatic, M. Nefovska, Dynamic analysis of steel frames with flexible connections, Comput. Struct. 80 (2002) 935–955.
[29] J. Da Silva, L. De Lima, PdS. Vellasco, S. De Andrade, R. De Castro, Nonlinear dynamic analysis of steel portal frames with semi-rigid connections, Eng. Struct. 30 (2008) 2566–2579.
[30] M. Ohsaki, T. Miyamura, M. Kohiyama, M. Hori, H. Noguchi, H. Akiba, et al., High-precision finite element analysis of elastoplastic dynamic responses of super-high-rise steel frames, Earthq. Eng. Struct. Dynam. 38 (2009) 635–654.
[31] J. Radnić, G. Baloević, D. Matešan, M. Smilović, On a numerical model for static and dynamic analysis of in-plane masonry infilled steel frames, Mater. Werkst. 44 (2013) 423–430.
[32] S. Moradi, M.S. Alam, B. Asgarian, Incremental dynamic analysis of steel frames equipped with NiTi shape memory alloy braces, Struct. Des. Tall Special Build. 23 (2014) 1406–1425.
[33] S.-W. Liu, R. Bai, S.-L. Chan, Dynamic Time-History Elastic Analysis of Steel Frames Using One Element Per Member, Elsevier, Structures, 2016, pp. 300–309.
[34] Y. Yu, X. Zhu, Nonlinear dynamic collapse analysis of semi-rigid steel frames based on the finite particle method, Eng. Struct. 118 (2016) 383–393.
[35] A.Q. Bhatti, Dynamic response characteristics of steel portal frames having semi-rigid joints under sinusoidal wave excitation, Int. J. Adv. Struct. Eng. 9 (2017) 309–313.
[36] M. Khorami, M. Khorami, H. Motahar, M. Alvansazyazdi, M. Shariati, A. Jalali, et al., Evaluation of the seismic performance of special moment frames using incremental nonlinear dynamic analysis, Struct. Eng. Mech. 63 (2017) 259–268.
[37] H. Far, Dynamic behaviour of unbraced steel frames resting on soft ground, Steel Construct. 12 (2019) 135–140.
[38] V. Sharma, M.K. Shrimali, S.D. Bharti, T.K. Datta, Behavior of semi-rigid steel frames under near-and far-field earthquakes, Steel Compos. Struct. 34 (2020) 625–641.
[39] S.-W. Liu, Y.-P. Liu, S.-L. Chan, Direct analysis by an arbitrarily-located-plastic-hinge element - Part 2: spatial analysis, J. Constr. Steel Res. 103 (2014) 316–326.
[40] S.-W. Liu, Y.-P. Liu, S.-L. Chan, Direct analysis by an arbitrarily-located-plastic-hinge element - Part 1: planar analysis, J. Constr. Steel Res. 103 (2014) 303–315.
[41] W.F. Chen, E.M. Lui, Structural Stability: Theory and Implementation, Elsevier, New York, 1987.
[42] S.G. Ekhande, M. Selvappalam, M.K.S. Madugula, Stability functions for three-dimensional beam-columns, J. Struct. Eng. 115 (1989) 467–479.
[43] R.D. Ziemian, W. McGuire, Modified tangent modulus approach, A contribution to plastic hinge analysis, J. Struct. Eng. 128 (2002) 1301–1307.
[44] S.I. Hilmy, J.F. Abel, Material and geometric nonlinear dynamic analysis of steel frames using computer graphics, Comput. Struct. 21 (1985) 825–840.
[45] ECCS, Ultimate limit state calculation of sway frames with rigid joints, in: Technical Committee 8 – Structural Stability Technical Working Group 8, European Convention for Constructional Steelwork, 1984, p. 2. System Publication No. 33.
[46] J.G. Orbison, W. McGuire, J.F. Abel, Yield surface applications in nonlinear steel frame analysis, Comput. Methods Appl. Mech. Eng. 33 (1982) 557–573.
[47] N.M. Newmark, A method of computation for structural dynamic, J. Eng. Mech. Div.-Asce. 85 (1959) 67–94.
[48] ABAQUS, Analysis User's Manual Version 6.14, Dassault Systems, 2014.
[49] SAP2000. CSI Analysis Reference Manual, Computers & Structures, Inc., 2017.
[50] PEER, The PEER Ground Motion Database, Pacific Earthquake Engineering Research Center, 2011. http://peer.berkeley.edu/peer_ground_motion_database/spectras/21713/unscaled_searches/new.
[51] A.K. Chopra, Dynamics of Structures: Theory and Applications to Earthquake Engineering, Pearson Prentice Hall, Upper Saddle River, New Jersey, 2007, p. 7458.